Visualizing and Steering Dissociative Frustrated Double Ionization of Hydrogen Molecules

Wenbin Zhang,[1] Zuqing Yu,[2] Xiaochun Gong,[1] Junping Wang,[2] Peifen Lu,[1] Hui Li,[1] Qiying Song,[1] Qinying Ji,[1] Kang Lin,[1] Junyang Ma,[1] Hanxiao Li,[1] Fenghao Sun,[1] Junjie Qiang,[1] Heping Zeng,[1] Feng He,[2,*] and Jian Wu[1,3,†]

[1]*State Key Laboratory of Precision Spectroscopy, East China Normal University, Shanghai 200062, China*

[2]*Key Laboratory of Laser Plasmas (Ministry of Education) and School of Physics and Astronomy, Collaborative Innovation Center for IFSA (CICIFSA), Shanghai Jiao Tong University, Shanghai 200240, China*

[3]*Collaborative Innovation Center of Extreme Optics, Shanxi University, Taiyuan, Shanxi 030006, China*

(Received 14 May 2017; revised manuscript received 29 August 2017; published 19 December 2017)

We experimentally visualize the dissociative frustrated double ionization of hydrogen molecules by using few-cycle laser pulses in a pump-probe scheme, in which process the tunneling ionized electron is recaptured by one of the outgoing nuclei of the breaking molecule. Three internuclear distances are recognized to enhance the dissociative frustrated double ionization of molecules at different instants after the first ionization step. The recapture of the electron can be further steered to one of the outgoing nuclei as desired by using phase-controlled two-color laser pulses. Both the experimental measurements and numerical simulations suggest that the Rydberg atom is favored to emit to the direction of the maximum of the asymmetric optical field. Our results on the one hand intuitively visualize the dissociative frustrated double ionization of molecules, and on the other hand open the possibility to selectively excite the heavy fragment ejected from a molecule.

DOI: 10.1103/PhysRevLett.119.253202

When exposed to strong laser fields, a wealth of fascinating phenomena are manifested in molecules such as the bond softening and hardening [1–4], the above-threshold dissociation [5,6], the Coulomb explosion [7–9], the directional bond breaking [10–15], and the charge-resonance-enhanced ionization (CREI) [16–19]. Besides the ionization, there is a certain probability for the neutral atoms to survive in strong laser fields [20,21], where the detached slow electrons would be eventually recaptured into Rydberg orbitals [22,23]. The Rydberg excitation plays important roles in the acceleration of neutral atoms [24], the formation of low-energy structures of photoelectrons [25–27], and the near-threshold harmonics generation [28].

For molecules in strong laser fields, a liberated electron can be recaptured by the ejected ionic fragments [29–31]. Taking the double ionization of hydrogen molecules as an example, one of the tunneling ionized electrons may be recaptured by one of the outgoing ionic cores, leading to the dissociative frustrated double ionization (FDI) [29], i.e., $H_2 + m\hbar\omega \rightarrow H^+ + H^+ + 2e \rightarrow H^+ + H^* + e$ denoted as (H^+, H^*) for H_2 or (D^+, D^*) for D_2 hereafter. Although the dissociative FDI channels were generally observed for various molecules [32–36], the most fundamental issues on when and where such process occurs stand yet experimentally unobserved. For the symmetric breaking of a doubly ionized diatomic homonuclear molecule, the recapture probability of the electron to two repulsive nuclei should be identical in general. The steering of the recapture of the electron to a desired ionic core, not realized yet, will open the possibility to selectively excite the heavy fragment into Rydberg states.

In this Letter, we real-time observe the dissociative FDI of hydrogen molecules by performing a few-cycle pump-probe measurement in a reaction microscope. The photoionization created ionic fragment, the excited Rydberg atom, and the freed electron ejected from the same molecule, are measured in coincidence to unambiguously identify the dissociative FDI channel. Three internuclear distances of the stretching molecular ion are recognized to enhance the dissociative FDI at different instants. By finely adjusting the phase of a two-color laser pulse, the recapture of the tunneling ionized electron to one of the outgoing ionic cores can be steered. This allows us to selectively excite the ejected neutral fragment from a breaking molecule by using waveform-controlled ultrashort laser pulses.

As schematically illustrated in Fig. 1(a), the measurements were performed in a reaction microscope of cold-target recoil-ion momentum spectroscopy (COLTRIMS) [37,38]. A linearly polarized femtosecond laser pulse (25 fs, 790 nm, 10 kHz) was either spectrally broadened in a gas-filled hollow-core fiber and afterwards temporally compressed to produce 7-fs few-cycle pulses for the pump-probe experiment, or frequency doubled in a β-barium borate (β-BBO) crystal to generate a two-color pulse in a collinear scheme [39] for the steering of the electron recapture dynamics. The relative phase ϕ_L between the fundamental wave (FW) and second-harmonic (SH) wave of the two-color pulse can be finely tuned by scanning the inset of a pair of fused-silica wedges. The laser pulses were

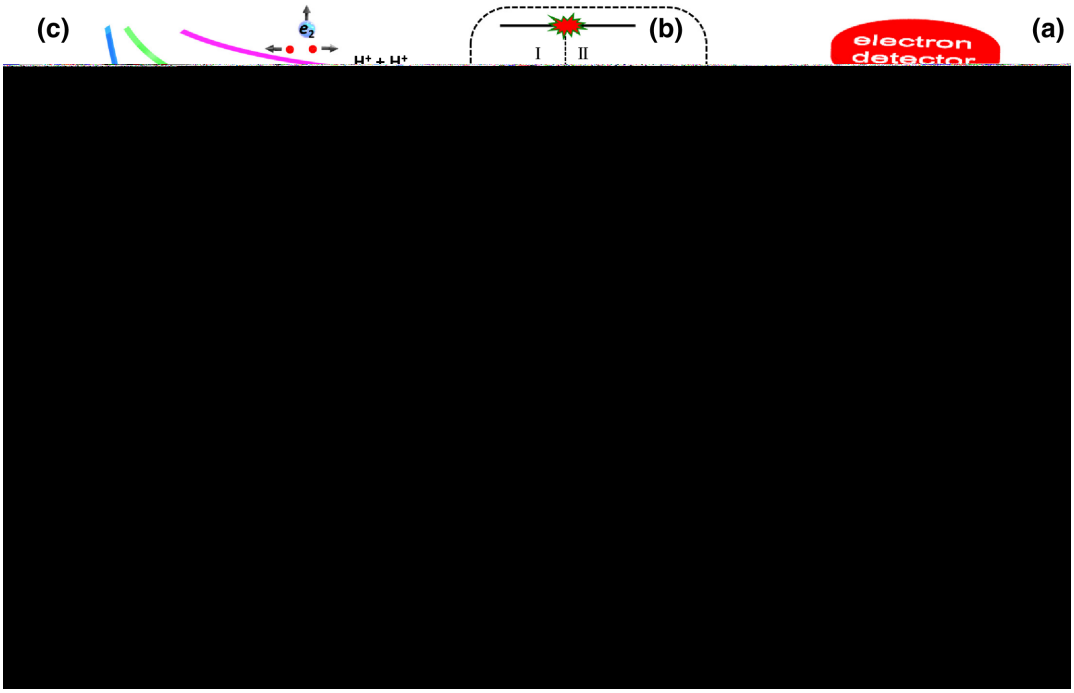

FIG. 1. (a) Schematic diagram of the experimental setup. (b) Illustration of the spectrometer configuration of the ion side of the COLTRIMS apparatus. (c) Schematic illustration of the stepwise dynamics of the dissociative FDI of H_2.

afterwards focused onto a supersonic gas jet of hydrogen molecules (H_2 or D_2) in the COLTRIMS. The laser intensities in the interaction region were measured to be 6.4×10^{14} W/cm^2 for the few-cycle pulses, and $I_{\mathrm{FW}} \sim 2.4 \times 10^{14}$ and $I_{\mathrm{SH}} \sim 0.42 \times 10^{14}$ W/cm^2 for the two-color fields, respectively. More details of the experimental method can be found in the Supplemental Material [40].

For dissociative FDI of hydrogen molecules, the produced ionic fragment (H^+ or D^+) accelerated by the static electric field of the spectrometer ($E_s \sim 12.7$ V/cm) can be detected by the ion detector regardless of its ejection direction. However, the laser-created Rydberg atom (H^* or D^*) can only be detected if it flies towards the ion detector and impinges on the microchannel plate (MCP) detector with an internal potential energy larger than the work function of the MCP [43]. Meanwhile, the freed electron accelerated by E_s and guided by a weak magnetic field ($B \sim 11$ G) can be detected by the electron detector at the other end of the spectrometer.

As shown in Fig. 2(a), we identify the (H^+, H^*) pair by using the photoion- photoion coincidence (PIPICO) spectrum of the heavy fragments. Because of the absence of the acceleration by E_s of the spectrometer, the neutral H^* flies to the ion detector with the mere momentum gained from the dissociation and exhibits a much larger time of flight (TOF) (between 1400 and 5500 ns in our experiments) as compared to that of H^+. The (H^+, H^*) pair is clearly distinguished from the Coulomb-exploded double ionization channel of (H^+, H^+), i.e., $H_2 + m\hbar\omega \rightarrow H^+ + H^+ + 2e$ in the PIPICO spectrum. By increasing E_s of the spectrometer, as expected, the TOF of the H^+ gradually decreases while the TOF of the H^* remains unshifted. We hence confirmed that the earlier and later arrived fragments of the (H^+, H^*) pair are the ionic and the neutral fragments,

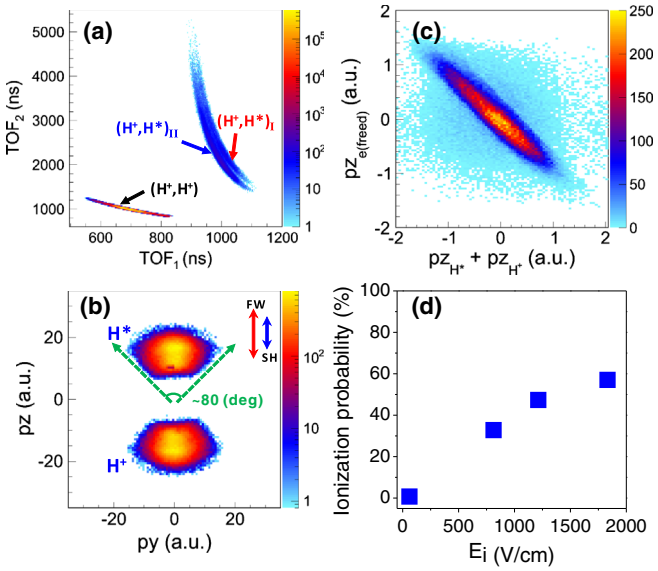

FIG. 2. (a) Measured PIPICO spectrum of the (H^+, H^+) and (H^+, H^*) channels. (b) Momentum distribution of the H^+ and H^* fragments of the (H^+, H^*) channel in the $y - z$ plane. (c) Momentum correlation map between the ionic H^+, neutral excited H^*, and the freed electron of the (H^+, H^*) channel along the time-of-flight direction of the spectrometer. (d) Measured ionization probability of the laser-created H^* as a function of the static electric field E_i.

respectively. As shown in Fig. 2(b), the H^* has a momentum similar to that of the H^+ but emits to the opposite direction. The geometrical acceptance for the detection of H^* in our experiments is about 0.9π sr. Since only the H^* having momentum closely parallel to the TOF direction of the spectrometer was collected, the measured yield ratio of $(H^+, H^*)/(H^+, H^+) \sim 1\%$ is underestimated as compared to the real events of the (H^+, H^*) generated in our experiment. As shown in Fig. 2(c), the momentum of the freed electron and the sum momentum of the H^+ and H^* concentrates along the diagonal line of the 2D spectrum by obeying the momentum conservation of the breaking molecule, which allows us to unambiguously identify the dissociative FDI channel.

The dual PIPICO lines of the (H^+, H^*) pair, i.e., the $(H^+, H^*)_{\mathrm{I}}$ and $(H^+, H^*)_{\mathrm{II}}$ in Fig. 2(a), are related to the field ionization of Rydberg atoms [44–46]. As illustrated in Fig. 1(b), the H^* survived from E_s ($\sim$12.7 V/cm) of the spectrometer can be detected by the MCP detector either as H^* or indirectly as H^+ after the field ionization and acceleration by the electric field E_i ($\sim$1500 V/cm) between the mesh and MCP. Therefore, the E_i-ionized H^* arrives at the detector earlier and is detected as H^+ to form the $(H^+, H^*)_{\mathrm{II}}$; while the survived H^* without ionization by E_i is recorded as the $(H^+, H^*)_{\mathrm{I}}$. For a Rydberg atom with principal quantum number of n, the threshold of the static electric field for field ionization obeys the scaling law $E_i = 1/(f_c n^4)$ ($2.6 \le f_c \le 7.7$ for a hydrogen atom) [47]. By adjusting the strength of E_i for fixed E_s, we measured the E_i-dependent ionization probability of the neutral H^*, i.e., the yield ratio of the ionized portion and the initial ensemble $R = N_{(H^+,H^*)\mathrm{II}}/[N_{(H^+,H^*)\mathrm{I}} + N_{(H^+,H^*)\mathrm{II}}]$, as shown in Fig. 2(d). Please note that this ratio is affected by the spontaneous decay of Rydberg atoms of low-n values on their way to the detector, which hampers the precise reconstruction of the initial distribution of n of the laser-created Rydberg atoms. We estimated an upper limit of $n \sim 40$ of the H^* of the (H^+, H^*) pair produced in our experiments.

In the following we first used few-cycle pump-probe pulses to learn about the dynamics of the dissociative FDI and then used the phase-controlled asymmetric two-color pulses to steer the recapture of the tunneling ionized electron. As illustrated in Fig. 1(c), the pump pulse frees an electron from the hydrogen molecule and launches a nuclear wave packet (NWP) onto the $1s\sigma_g$ state of the molecular ion. The created NWP may up and down transit between the $1s\sigma_g$ and $2p\sigma_u$ states coupled by the laser field when it propagates outwards [48]. As the stretching molecular ion passes through the critical range of internuclear distance R_c, the CREI of the molecular ion occurs by releasing the second electron. However, there is a certain probability that the freed electron is recaptured into Rydberg orbitals of one of the outgoing ionic cores driven by the time-delayed probe pulse. By tuning the time delay

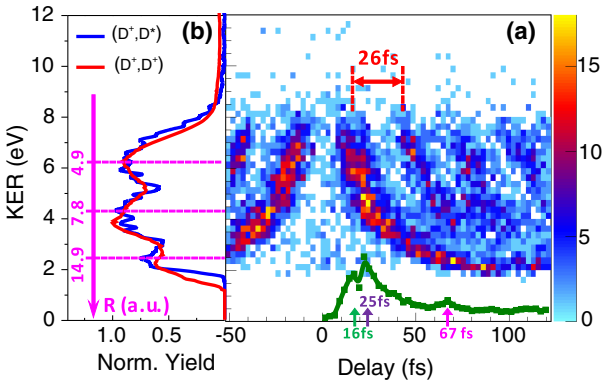

FIG. 3. (a) Measured time-delay-dependent KER spectrum of the (D^+, D^*) channel driven by few-cycle pump and probe pulses. The green curve at the bottom of the panel shows the (D^+, D^*) yield versus the pump-probe time delay for the first KER stripe at positive time delay. (b) The KER spectra of the (D^+, D^*) and (D^+, D^+) channels by integrating over all the time delay.

of the probe pulse [48,49], we real-time visualize the dissociative FDI of molecules. For instance, by tracing the delay-dependent kinetic energy release (KER) of the ejected nuclei, one may identify the time after the first ionization step and the internuclear distance of the stretching molecular ion at which the second electron is tunneled but eventually recaptured. To readily resolve the time-dependent structure, D_2 is used as the target molecule in the pump-probe measurement for its relative slow vibrational motion.

Figure 3(a) displays the measured KER spectrum of the (D^+, D^*) channel as a function of the time delay between the few-cycle pump and probe pulses, where three distinct features can be distinguished. First, the (D^+, D^*) channel nearly vanishes around the zero time delay, but only becomes visible when the time delay is increased to $\tau \sim 7$ fs. It indicates that the dissociative FDI is favored at a large internuclear distance of the stretching molecular ion. This is consistent with the fact that the (D^+, D^*) channel is negligible in a single beam of few-cycle pulses in our experiment. Second, periodical stripes with an interval of $\sim$26 fs appear in the time-dependent KER spectrum, corresponding to the vibrational oscillation of the NWP on the bound state of the molecular ion. A portion of the NWP dissociates when it approaches the outer turning point of the bound sate and is afterwards field excited to produce the (D^+, D^*) channel by the time delayed probe pulse. Third, fine structures show up in each individual time-dependent KER stripe. The KER of the (D^+, D^*) maps the internuclear separation R at the instant of the excitation by the time delayed probe pulse. As indicated by the vertical arrows in Fig. 3(a), the yield of the (D^+, D^*) channel is enhanced when the probe pulse arrives at around $\tau \sim 16$, 25, and 67 fs, which corresponds to the KER peaks around 6.3, 4.2, and 2.5 eV shown in Fig. 3(b), respectively. Since the high-lying Rydberg states are very close to the Coulombic

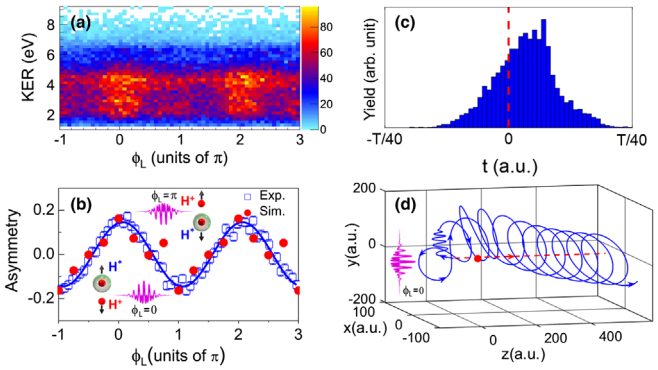

FIG. 4. (a) Measured phase-dependent KER spectrum of the (H^+, H^*) channel in a linearly polarized two-color laser pulse. (b) Asymmetry of the directional emission of H^* of the (H^+, H^*) channel versus the relative phase of the two-color laser pulse from the measurement (blue squares, KER integrated) and from the simulations (red circles). The solid curve is the numerical fit of the experimental data. (c) The simulated normalized probability of the electron to be recaptured as a function of the releasing time within the vicinity around the peak of an optical cycle. (d) A typical trajectory of the liberated electron, which is eventually captured by the $+z$-going nucleus in a z-polarized two-color pulse at $\phi_L = 0$, where the red dot denotes the $+z$-going nucleus. The red dashed arrow sketches the trajectory of the outgoing nucleus in the $+z$ direction.

repulsive curve of $1/R$, the KER spectrum of the (D^+, D^*) channel is similar to that of the (D^+, D^+) channel as plotted in Fig. 3(b). By assuming $\mathrm{KER}(\tau) = 1/R(\tau) + E_0$, the corresponding internuclear distances of the stretching molecular ion for enhanced ionization are estimated to be $R \sim 4.9$, 7.8, and 14.9 a.u., respectively. Here $E_0 = 0.7$ eV is the initial kinetic energy of the NWP at the tunneling instant of the second electron, which equals to the measured KER of the bond softening channel in the same experiment.

Based on the knowledge of the dynamics of the dissociative FDI, we will now test the possibility to steer the recapture of the tunneling ionized electron to one of the outgoing ionic cores of the breaking hydrogen molecule, e.g., H_2, by using a phase-controlled two-color laser pulse. As shown in Fig. 4(a), the yield of the (H^+, H^*) pair oscillates as a function of the relative phase ϕ_L of the two-color pulse, which weakly depends on the KER of the heavy fragments. Since only the H^* flying towards the ion detector could be measured in our experimental configuration, the yield modulation of the (H^+, H^*) pair stands for the directional ejection of the H^*. For quantification, as shown in Fig. 4(b), the directional emission of H^* is calculated by the differentially normalized asymmetry parameter $A(\phi_L) = [N(\phi_L) - N(\phi_L + \pi)]/[N(\phi_L) + N(\phi_L + \pi)]$, where $N(\phi_L)$ and $N(\phi_L + \pi)$ are the (H^+, H^*) yields at laser phases of ϕ_L and $\phi_L + \pi$, respectively. The positive or negative values of $A(\phi_L)$ stand for the favorable emission of the H^* towards or opposites to the ion detector. The amplitude of the asymmetric emission of H^* is about 20%. The ϕ_L-dependent asymmetry indicates that the laser created H^* mostly emits to the direction of the maximum of the asymmetric optical field as schematically illustrated in Fig. 4(b).

To unveil the ϕ_L-dependent directional electron recapture leading to the asymmetric emission of H^*, we traced the electron motion in the combined laser and Coulomb fields by performing classical trajectory Monte Carlo (CTMC) simulations [29]. In the scenario of the CREI [16–19], the electron in the up-field core is favored to overcome the narrow interatomic Coulomb barrier and released. In simulations, we put the electron ensemble weighted by the time-dependent Ammosov-Delone-Krainov rate in the middle of the two nuclei, and afterwards propagated the classical ensemble in the two-color laser and Coulomb fields [29]. Meanwhile, two nuclei move repulsively with an initial relative velocity of 0.02 a.u. and an initial internuclear distance of 8 a.u.. Finally, we collected electrons having energies in the range of $[-0.1, 0]$ a.u., which were regarded as electrons in Rydberg orbitals, and calculated the asymmetric distribution on two nuclei with the same manner done in experiment. More details of the simulation method can be found in the Supplemental Material [40]. The calculated asymmetries of the directional emission of H^* are shown in Fig. 4(b) (red circles), which agree with the experimental measurement reasonably well.

The CTMC simulations allow us to get intuitive insights of the fundamental mechanism of the asymmetric electron recapture. For instance, at $\phi_L = 0$, the electron tunnels out around the peak of the laser electric field. Figure 4(c) shows the probability of the electron recaptured by the nuclei as a function of the releasing time within the vicinity around the peak of an optical cycle. Partitioned by the vertical dashed line, the electrons emitting after the peak exhibit larger probabilities to be ultimately recaptured by the nuclei as compared to those emitting before the laser peak. The asymmetric distribution with respect to this vertical dashed line is due to the different Coulomb actions of the ion on the electrons emitting before or after the field maximum. The electrons released after the peak of the optical field will finally acquire a drift velocity in the $+z$ direction, and these electrons are prone to be recaptured by the parallel- rather than the antiparallel-propagating nucleus. A typical trajectory of the recaptured electron is shown in Fig. 4(d), in which the electron first moves to the down-field core, then surrounds the two nuclei, but finally orbits the $+z$-going nucleus with a radius around ~100 a.u.

The here-observed directional emission of H^* in the dissociative FDI of H_2 differs from the asymmetric electron localization in the dissociative single ionization of hydrogen molecules [10–15], where the asymmetry is governed by the mixture of two lowest electronic bound states having opposite parities. For the dissociative FDI of H_2, the H_2^+

created in the first ionization step is favored to be ionized by releasing the second electron around the critical internuclear distance of the stretching molecular ion. A portion of the freed electrons flying together with one of the outgoing nuclei will be recaptured into the Rydberg orbitals by the corresponding core to form H^*. Depending on the correlation of the freed electron and the dissociative heavy fragments, the asymmetric formation of H^* can be steered by controlling the phase of a two-color pulse, which, however, very weakly depends on the KER of the (H^+, H^*) pair as compared to the asymmetric electron localization [10–15].

In summary, we experimentally real-time visualized the dynamics of dissociative FDI of hydrogen molecules by using few-cycle pump and probe pulses, and meanwhile demonstrated the steering of the recapture of the tunneling ionized electron to a desired ionic core of the breaking molecule by using phase-controlled two-color pulses. Our results not only strengthen the understanding of the mechanism of the dissociative FDI of molecules, but also open the possibility to selectively excite the neutral fragment ejected from a breaking molecule. The present study will stimulate further investigations on the strong-field frustrated ionization of molecules for various applications.

This work is supported by the National Natural Science Foundation of China (Grants No. 11425416, No. 61690224, No. 11621404, No. 11322438, No. 11574205, No. 11421064), The 111 Project of China (Grant No. B12024), and the Outstanding Doctoral Dissertation Cultivation Plan of Action (YB2016036) and Innovation Program of Shanghai Municipal Education Commission (2017-01-07-00-02-E00034). Simulations were performed on the π supercomputer at Shanghai Jiao Tong University.

*fhe@sjtu.edu.cn
†jwu@phy.ecnu.edu.cn

[1] P. H. Bucksbaum, A. Zavriyev, H. G. Muller, and D. W. Schumacher, Phys. Rev. Lett. **64**, 1883 (1990).
[2] M. Magrakvelidze, F. He, T. Niederhausen, I. V. Litvinyuk, and U. Thumm, Phys. Rev. A **79**, 033410 (2009).
[3] L. J. Frasinski, J. H. Posthumus, J. Plumridge, K. Codling, P. F. Taday, and A. J. Langley, Phys. Rev. Lett. **83**, 3625 (1999).
[4] G. Yao and S.-I. Chu, Phys. Rev. A **48**, 485 (1993).
[5] A. Giusti-Suzor, X. He, O. Atabek, and F. H. Mies, Phys. Rev. Lett. **64**, 515 (1990).
[6] G. Jolicard and O. Atabek, Phys. Rev. A **46**, 5845 (1992).
[7] H. Stapelfeldt, E. Constant, and P. B. Corkum, Phys. Rev. Lett. **74**, 3780 (1995).
[8] B. D. Esry, A. M. Sayler, P. Q. Wang, K. D. Carnes, and I. Ben-Itzhak, Phys. Rev. Lett. **97**, 013003 (2006).
[9] A. Hishikawa, A. Iwamae, K. Hoshina, M. Kono, and K. Yamanouchi, Chem. Phys. **231**, 315 (1998).
[10] M. F. Kling, Ch. Siedschlag, A. J. Verhoef, J. I. Khan, M. Schultze, Th. Uphues, Y. Ni, M. Uiberacker, M. Drescher, F. Krausz, and M. J. J. Vrakking, Science **312**, 246 (2006).
[11] M. Kremer, B. Fischer, B. Feuerstein, V. L. B. de Jesus, V. Sharma, C. Hofrichter, A. Rudenko, U. Thumm, C. D. Schröter, R. Moshammer, and J. Ullrich, Phys. Rev. Lett. **103**, 213003 (2009).
[12] D. Ray, F. He, S. De, W. Cao, H. Mashiko, P. Ranitovic, K. P. Singh, I. Znakovskaya, U. Thumm, G. G. Paulus, M. F. Kling, I. V. Litvinyuk, and C. L. Cocke, Phys. Rev. Lett. **103**, 223201 (2009).
[13] J. McKenna, F. Anis, A. M. Sayler, B. Gaire, N. G. Johnson, E. Parke, K. D. Carnes, B. D. Esry, and I. Ben-Itzhak, Phys. Rev. A **85**, 023405 (2012).
[14] J. Wu, M. Magrakvelidze, L. P. H. Schmidt, M. Kunitski, T. Pfeifer, M. Schöffler, M. Pitzer, M. Richter, S. Voss, H. Sann, H. Kim, J. Lower, T. Jahnke, A. Czasch, U. Thumm, and R. Dörner, Nat. Commun. **4**, 2177 (2013).
[15] X. Gong, P. He, Q. Song, Q. Ji, H. Pan, J. Ding, F. He, H. Zeng, and J. Wu, Phys. Rev. Lett. **113**, 203001 (2014).
[16] T. Zuo and A. D. Bandrauk, Phys. Rev. A **52**, R2511 (1995).
[17] S. Chelkowski, A. D. Bandrauk, A. Staudte, and P. B. Corkum, Phys. Rev. A **76**, 013405 (2007).
[18] J. Wu, M. Meckel, L. Ph. H. Schmidt, M. Kunitski, S. Voss, H. Sann, H. Kim, T. Jahnke, A. Czasch, and R. Dörner, Nat. Commun. **3**, 1113 (2012).
[19] X. Gong, Q. Song, Q. Ji, H. Pan, J. Ding, J. Wu, and H. Zeng, Phys. Rev. Lett. **112**, 243001 (2014).
[20] M. P. de Boer and H. G. Muller, Phys. Rev. Lett. **68**, 2747 (1992).
[21] R. R. Jones, D. W. Schumacher, and P. H. Bucksbaum, Phys. Rev. A **47**, R49 (1993).
[22] T. Nubbemeyer, K. Gorling, A. Saenz, U. Eichmann, and W. Sandner, Phys. Rev. Lett. **101**, 233001 (2008).
[23] S. Larimian, C. Lemell, V. Stummer, J. W. Geng, S. Roither, D. Kartashov, L. Zhang, M. X. Wang, Q. Gong, L. Y. Peng, S. Yoshida, J. Burgdörfer, A. Baltuška, M. Kitzler, and X. Xie, Phys. Rev. A **96**, 021403(R) (2017).
[24] U. Eichmann, T. Nubbemeyer, H. Rottke, and W. Sandner, Nature (London) **461**, 1261 (2009).
[25] A. von Veltheim, B. Manschwetus, W. Quan, B. Borchers, G. Steinmeyer, H. Rottke, and W. Sandner, Phys. Rev. Lett. **110**, 023001 (2013).
[26] B. Wolter, C. Lemell, M. Baudisch, M. G. Pullen, X.-M. Tong, M. Hemmer, A. Senftleben, C. D. Schröter, J. Ullrich, R. Moshammer, J. Biegert, and J. Burgdörfer, Phys. Rev. A **90**, 063424 (2014).
[27] H. Liu, Y. Liu, L. Fu, G. Xin, D. Ye, J. Liu, X. T. He, Y. Yang, X. Liu, Y. Deng, C. Wu, and Q. Gong, Phys. Rev. Lett. **109**, 093001 (2012).
[28] W. H. Xiong, J. W. Geng, J. Y. Tang, L. Y. Peng, and Q. Gong, Phys. Rev. Lett. **112**, 233001 (2014).
[29] B. Manschwetus, T. Nubbemeyer, K. Gorling, G. Steinmeyer, U. Eichmann, H. Rottke, and W. Sandner, Phys. Rev. Lett. **102**, 113002 (2009).
[30] K. N. Shomsky, Z. S. Smith, and S. L. Haan, Phys. Rev. A **79**, 061402(R) (2009).

[31] A. Emmanouilidou, C. Lazarou, A. Staudte, and U. Eichmann, Phys. Rev. A **85**, 011402(R) (2012).
[32] T. Nubbemeyer, U. Eichmann, and W. Sandner, J. Phys. B **42**, 134010 (2009).
[33] J. McKenna, S. Zeng, J. J. Hua, A. M. Sayler, M. Zohrabi, Nora G. Johnson, B. Gaire, K. D. Carnes, B. D. Esry, and I. Ben-Itzhak, Phys. Rev. A **84**, 043425 (2011).
[34] B. Ulrich, A. Vredenborg, A. Malakzadeh, M. Meckel, K. Cole, M. Smolarski, Z. Chang, T. Jahnke, and R. Dörner, Phys. Rev. A **82**, 013412 (2010).
[35] B. Manschwetus, H. Rottke, G. Steinmeyer, L. Foucar, A. Czasch, H. Schmidt-Böcking, and W. Sandner, Phys. Rev. A **82**, 013413 (2010).
[36] J. Wu, A. Vredenborg, B. Ulrich, L. Ph. H. Schmidt, M. Meckel, S. Voss, H. Sann, H. Kim, T. Jahnke, and R. Dorner, Phys. Rev. Lett. **107**, 043003 (2011).
[37] R. Dörner, V. Mergel, O. Jagutzki, L. Spielberger, J. Ullrich, R. Moshammer, and H. Schmidt-Böcking, Phys. Rep. **330**, 95 (2000).
[38] J. Ullrich, R. Moshammer, A. Dorn, R. Dörner, L. P. H. Schmidt, and H. Schmidt-Böcking, Rep. Prog. Phys. **66**, 1463 (2003).
[39] J. Wu, A. Vredenborg, L. Ph. H. Schmidt, T. Jahnke, A. Czasch, and R. Dörner, Phys. Rev. A **87**, 023406 (2013).
[40] See Supplemental Material at http://link.aps.org/supplemental/10.1103/PhysRevLett.119.253202 for details of the experimental and simulation methods, which includes Refs. [41,42].
[41] A. S. Landsman, C. Hofmann, A. N. Pfeiffer, C. Cirelli, and U. Keller, Phys. Rev. Lett. **111**, 263001 (2013).
[42] J. Wu, L. Ph. H. Schmidt, M. Kunitski, M. Meckel, S. Voss, H. Sann, H. Kim, T. Jahnke, A. Czasch, and R. Dörner, Phys. Rev. Lett. **108**, 183001 (2012).
[43] Ben Berry, M. Zohrabi, D. Hayes, U. Ablikim, Bethany Jochim, T. Severt, K. D. Carnes, and I. Ben-Itzhak, Rev. Sci. Instrum. **86**, 046103 (2015).
[44] E. Diesen, U. Saalmann, M. Richter, M. Kunitski, R. Dörner, and J. M. Rost, Phys. Rev. Lett. **116**, 143006 (2016).
[45] H. Lv, W. Zuo, L. Zhao, H. Xu, M. Jin, D. Ding, S. Hu, and J. Chen, Phys. Rev. A **93**, 033415 (2016).
[46] S. Larimian, S. Erattupuzha, C. Lemell, S. Yoshida, S. Nagele, R. Maurer, A. Baltuška, J. Burgdörfer, M. Kitzler, and X. Xie, Phys. Rev. A **94**, 033401 (2016).
[47] M. J. Rakovic and S.-I. Chu, J. Phys. B **31**, 1989 (1998).
[48] Th. Ergler, A. Rudenko, B. Feuersvein, K. Zrost, C. D. Schröter, R. Moshammer, and J. Ullrich, Phys. Rev. Lett. **95**, 093001 (2005).
[49] A. S. Alnaser, B. Ulrich, X. M. Tong, I. V. Litvinyuk, C. M. Maharjan, P. Ranitovic, T. Osipov, R. Ali, S. Ghimire, Z. Chang, C. D. Lin, and C. L. Cocke, Phys. Rev. A **72**, 030702(R) (2005).